

**Analysis of PM<sub>10</sub> concentrations in Nelson Airshed B**

T. Ancelet

Authors

P. K. Davy

W. J. Trompetter

**GNS Science Consultancy Report 2013/47**

**April 2013**

### **DISCLAIMER**

This report has been prepared by the Institute of Geological and Nuclear Sciences Limited (GNS Science) exclusively for and under contract to Nelson City Council. Unless otherwise agreed in writing by GNS Science, GNS Science accepts no responsibility for any use of, or reliance on any contents of this Report by any person other than Nelson City Council and shall not be liable to any person other than Nelson City Council, on any ground, for any loss, damage or expense arising from such use or reliance.

The data presented in this Report are available to GNS Science for other use from May 2013.

### **BIBLIOGRAPHIC REFERENCE**

Ancelet, T. A.; Davy, P. K.; Trompetter, W. J. 2013. Analysis of PM<sub>10</sub> concentrations in Nelson Airshed B, *GNS Science Consultancy Report 2013/47*. 23 p.

## CONTENTS

<b>EXECUTIVE SUMMARY</b> .....	<b>III</b>
<b>1.0 INTRODUCTION</b> .....	<b>1</b>
1.1 Requirement to manage airborne particle pollution .....	1
1.2 Identifying the source(s) responsible for PM <sub>10</sub> concentrations.....	1
1.3 Report structure.....	2
<b>2.0 METHODOLOGY</b> .....	<b>3</b>
2.1 Data analysis .....	3
<b>3.0 TAHUNANUI MONITORING SITE</b> .....	<b>5</b>
3.1 Site description .....	5
3.2 PM <sub>10</sub> concentrations at the monitoring site .....	6
3.3 Local meteorology at the Tahunanui site .....	8
<b>4.0 ANALYSES OF POLLUTION EPISODES</b> .....	<b>10</b>
4.1 Analysis of PM <sub>10</sub> and meteorological data .....	10
4.2 Analysis using source apportionment study results .....	16
4.3 Implications for Nelson City Council.....	21
<b>5.0 SUMMARY OF THE ANALYSIS OF PM<sub>10</sub> CONCENTRATIONS AT TAHUNANUI</b> ..	<b>22</b>
<b>6.0 REFERENCES</b> .....	<b>23</b>

## FIGURES

Figure 1	Average hourly PM <sub>10</sub> concentrations ( $\mu\text{g m}^{-3}$ ) under southwest winds with wind speeds greater than $3 \text{ m s}^{-1}$ (blue) and all other wind speeds and directions (red) during each day of the week (a), overall average hourly PM <sub>10</sub> concentrations ( $\mu\text{g m}^{-3}$ ) (b), average PM <sub>10</sub> concentrations ( $\mu\text{g m}^{-3}$ ) by month (c), and average PM <sub>10</sub> concentrations ( $\mu\text{g m}^{-3}$ ) by day of the week (d) Light shading indicates the 95% confidence intervals.....	iv
Figure 2	Scatterplot of motor vehicle and soil contributions combined ( $\mu\text{g m}^{-3}$ ) versus PM <sub>10</sub> concentrations ( $\mu\text{g m}^{-3}$ ) under winds from the southwest (blue) and all other wind quadrants (red).....	v
Figure 2.1	Location of the Tahunanui monitoring site in Nelson (★) (Source: Wisers Maps <a href="http://www.wises.co.nz">www.wises.co.nz</a> ).....	3
Figure 3.1	Map showing the location of the Tahunanui monitoring site (★) (Source: Wisers Maps <a href="http://www.wises.co.nz">www.wises.co.nz</a> ).....	5
Figure 3.2	Aerial view of the NCC monitoring site (Source: Google Earth 2013). .....	6
Figure 3.3	Hourly BAM PM <sub>10</sub> concentrations ( $\mu\text{g m}^{-3}$ ) at the Tahunanui site (data supplied by NCC). .....	7
Figure 3.4	Daily BAM PM <sub>10</sub> concentrations ( $\mu\text{g m}^{-3}$ ) at the Tahunanui site. The hashed line indicates the NES value ( $50 \mu\text{g m}^{-3}$ ). .....	7
Figure 3.5	Wind rose at Tahunanui from 2007–2012. ....	8
Figure 3.6	Wind roses at Tahunanui by season. ....	9
Figure 4.1	Average hourly PM <sub>10</sub> concentrations ( $\mu\text{g m}^{-3}$ ) during each day of the week (a), overall average hourly PM <sub>10</sub> concentrations ( $\mu\text{g m}^{-3}$ ) (b), average PM <sub>10</sub> concentrations ( $\mu\text{g m}^{-3}$ )	

	by month (c), and average PM <sub>10</sub> concentrations ( $\mu\text{g m}^{-3}$ ) by day of the week (d). Light shading indicates the 95% confidence intervals.....	11
Figure 4.2	Wintertime average hourly PM <sub>10</sub> concentrations ( $\mu\text{g m}^{-3}$ ) during each day of the week (a), wintertime average hourly PM <sub>10</sub> concentrations ( $\mu\text{g m}^{-3}$ ) (b), average PM <sub>10</sub> concentrations ( $\mu\text{g m}^{-3}$ ) by month (c), and average wintertime PM <sub>10</sub> concentrations ( $\mu\text{g m}^{-3}$ ) by day of the week (d). Light shading indicates the 95% confidence intervals.....	12
Figure 4.3	Southwesterly winds: Average hourly PM <sub>10</sub> concentrations ( $\mu\text{g m}^{-3}$ ) during each day of the week (a), overall average hourly PM <sub>10</sub> concentrations ( $\mu\text{g m}^{-3}$ ) (b), average PM <sub>10</sub> concentrations ( $\mu\text{g m}^{-3}$ ) by month (c), and average PM <sub>10</sub> concentrations ( $\mu\text{g m}^{-3}$ ) by day of the week (d) when winds were from the southwest quadrant (180–270°). Light shading indicates the 95% confidence intervals.....	13
Figure 4.4	Northeasterly, northwesterly and southeasterly winds: Average hourly PM <sub>10</sub> concentrations ( $\mu\text{g m}^{-3}$ ) during each day of the week (a), overall average hourly PM <sub>10</sub> concentrations ( $\mu\text{g m}^{-3}$ ) (b), average PM <sub>10</sub> concentrations ( $\mu\text{g m}^{-3}$ ) by month (c), and average PM <sub>10</sub> concentrations ( $\mu\text{g m}^{-3}$ ) by day of the week (d) when winds were from the NE, NW and SE quadrants (0–180 and 270–360°). Light shading indicates the 95% confidence intervals.....	14
Figure 4.5	Average hourly PM <sub>10</sub> concentrations ( $\mu\text{g m}^{-3}$ ) under southwest winds with wind speeds greater than $3 \text{ m s}^{-1}$ during each day of the week (a), overall average hourly PM <sub>10</sub> concentrations ( $\mu\text{g m}^{-3}$ ) (b), average PM <sub>10</sub> concentrations ( $\mu\text{g m}^{-3}$ ) by month (c), and average PM <sub>10</sub> concentrations ( $\mu\text{g m}^{-3}$ ) by day of the week (d) Light shading indicates the 95% confidence intervals.....	15
Figure 4.6	Average hourly PM <sub>10</sub> concentrations ( $\mu\text{g m}^{-3}$ ) under southwest winds with wind speeds greater than $3 \text{ m s}^{-1}$ (blue) and all other wind speeds and directions (red) during each day of the week (a), overall average hourly PM <sub>10</sub> concentrations ( $\mu\text{g m}^{-3}$ ) (b), average PM <sub>10</sub> concentrations ( $\mu\text{g m}^{-3}$ ) by month (c), and average PM <sub>10</sub> concentrations ( $\mu\text{g m}^{-3}$ ) by day of the week (d) Light shading indicates the 95% confidence intervals.....	16
Figure 4.7	Scatterplot of motor vehicle contributions ( $\mu\text{g m}^{-3}$ ) versus PM <sub>10</sub> concentrations ( $\mu\text{g m}^{-3}$ ) under winds from the southwest (blue) and all other wind quadrants (red). .....	17
Figure 4.8	Scatterplot of soil contributions ( $\mu\text{g m}^{-3}$ ) versus PM <sub>10</sub> concentrations ( $\mu\text{g m}^{-3}$ ) under winds from the southwest (blue) and all other wind quadrants (red). .....	18
Figure 4.9	Scatterplot of sulphate contributions ( $\mu\text{g m}^{-3}$ ) versus PM <sub>10</sub> concentrations ( $\mu\text{g m}^{-3}$ ) under winds from the southwest (blue) and all other wind quadrants (red). .....	18
Figure 4.10	Scatterplot of surface coating activity contributions ( $\mu\text{g m}^{-3}$ ) versus PM <sub>10</sub> concentrations ( $\mu\text{g m}^{-3}$ ) under winds from the southwest (blue) and all other wind quadrants (red).....	19
Figure 4.11	Scatterplot of motor vehicle and soil contributions combined ( $\mu\text{g m}^{-3}$ ) versus PM <sub>10</sub> concentrations ( $\mu\text{g m}^{-3}$ ) under winds from the southwest (blue) and all other wind quadrants (red).....	20
Figure 4.12	Scatterplot of soil contributions ( $\text{ng m}^{-3}$ ) calculated from mass reconstruction versus PM <sub>10</sub> concentrations ( $\mu\text{g m}^{-3}$ ) under winds from the southwest (blue) and all other wind quadrants (red).....	20

## EXECUTIVE SUMMARY

A study of peak PM<sub>10</sub> concentrations experienced at an ambient air quality monitoring site at Tahunanui in Nelson Airshed B has provided important and highly relevant information for the management of air quality by Nelson City Council. This report presents the results of an investigation of non-winter peak PM<sub>10</sub> concentrations that lead to occasional breaches of the National Environmental Standard for air quality at Tahunanui in Nelson Airshed B. PM<sub>10</sub> concentration and meteorological data from 2008–2012 were used in conjunction with results from a 2010 receptor modeling study to determine the source(s) responsible for the high PM<sub>10</sub> concentrations that occur under moderate to high wind speeds from the southwest.

Key results from the study are:

1. PM<sub>10</sub> concentrations under moderate to high speed winds from the southwest show a strong workday peak and strong weekday/weekend differences, with peak PM<sub>10</sub> concentrations occurring throughout the week between 6am and 6pm (Figure 1).
2. PM<sub>10</sub> compositional data and the results from a receptor modelling study showed that motor vehicle emissions and crustal matter (soil) contributions to PM<sub>10</sub> were the only sources well-correlated with southwesterly winds, indicating that vehicular movements and wind-blown dust in an industrial area to the southwest of the Tahunanui monitoring site were likely to be responsible for the peak PM<sub>10</sub> concentrations (Figure 2).

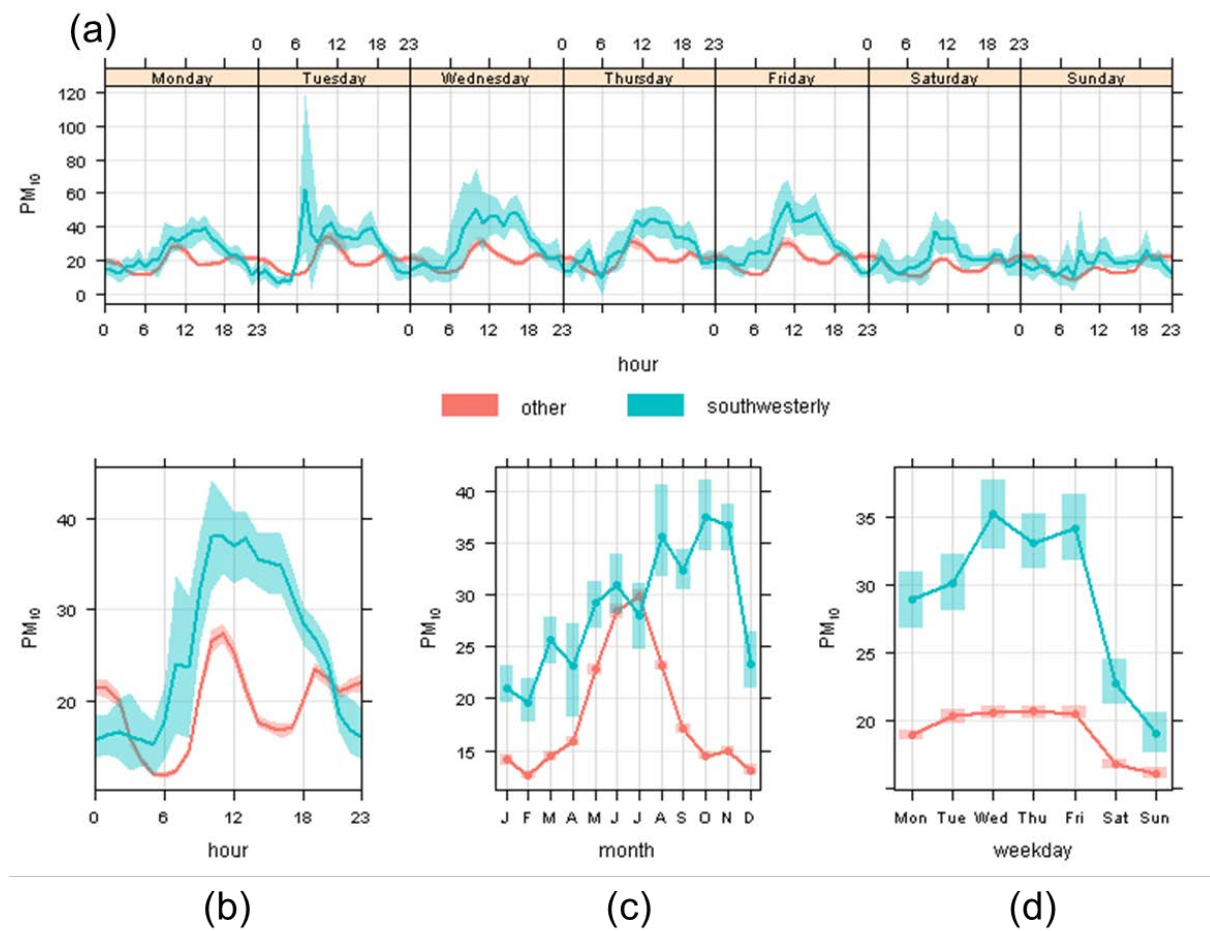


Figure 1 Average hourly PM<sub>10</sub> concentrations (µg m<sup>-3</sup>) under southwest winds with wind speeds greater than 3 m s<sup>-1</sup> (blue) and all other wind speeds and directions (red) during each day of the week (a), overall average hourly PM<sub>10</sub> concentrations (µg m<sup>-3</sup>) (b), average PM<sub>10</sub> concentrations (µg m<sup>-3</sup>) by month (c), and average PM<sub>10</sub> concentrations (µg m<sup>-3</sup>) by day of the week (d) Light shading indicates the 95% confidence intervals.

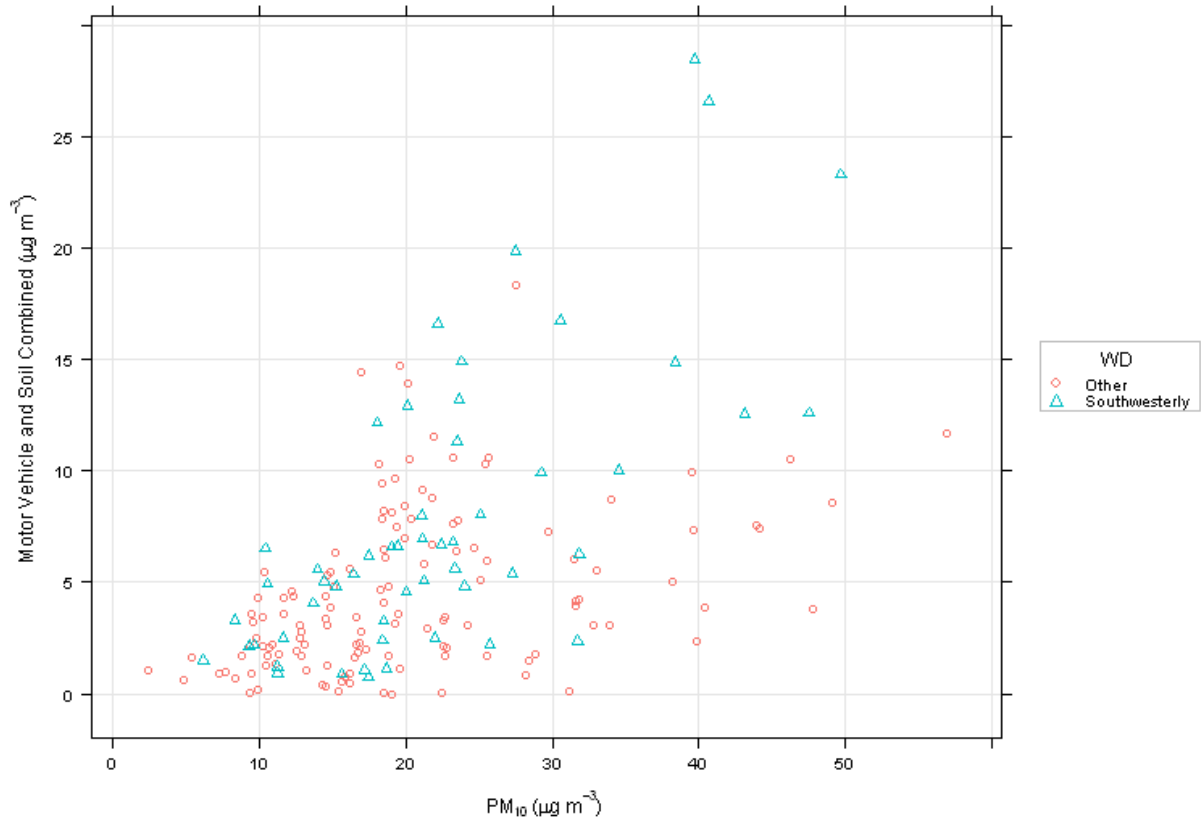


Figure 2 Scatterplot of motor vehicle and soil contributions combined ( $\mu\text{g m}^{-3}$ ) versus  $\text{PM}_{10}$  concentrations ( $\mu\text{g m}^{-3}$ ) under winds from the southwest (blue) and all other wind quadrants (red).





## 1.0 INTRODUCTION

This report presents results from an investigation of peak non-winter PM<sub>10</sub> concentrations measured at an ambient air quality monitoring site at Tahunanui, in Nelson Airshed B. These PM<sub>10</sub> excursions occasionally breach the National Environmental Standard for Air Quality (NES) (50 µg m<sup>-3</sup> for PM<sub>10</sub>). This work was commissioned by the Nelson City Council (NCC) as part of their ambient air quality monitoring strategy and was partly funded by an Envirolink grant (NLCC 67) from the Ministry of Business, Innovation and Employment.

### 1.1 REQUIREMENT TO MANAGE AIRBORNE PARTICLE POLLUTION

In response to growing evidence of significant health effects associated with airborne particle pollution, the New Zealand Government introduced a National Environmental Standard (NES) in 2005 of 50 µg m<sup>-3</sup> for particles less than 10 µm in aerodynamic diameter (denoted as PM<sub>10</sub>). The NES places an onus on regional councils to monitor PM<sub>10</sub> and publicly report if the air quality in their region exceeds the standard. Initially, regional councils were required to comply with the standard by 2013 or face restrictions on the granting of resource consents for discharges that contain PM<sub>10</sub>, but the NES has since been revised, extending the target date for regional councils to comply with the standard. The new target dates are September 1, 2016 for airsheds with between 1 and 10 exceedances and September 1, 2020 for airsheds with 10 or more exceedances. In areas where the PM<sub>10</sub> standard is exceeded, information on the sources contributing to those air pollution episodes is required to effectively manage air quality and formulate appropriate mitigation strategies.

### 1.2 IDENTIFYING THE SOURCE(S) RESPONSIBLE FOR PM<sub>10</sub> CONCENTRATIONS

Simply measuring the mass concentration of particulate matter (PM) provides little information about the contributing sources. However, detailed analyses of the spatial, temporal and meteorological conditions that result in peak PM concentrations can provide important insights into the nature of the offending source or sources. For example, time-series and meteorological analyses indicating that PM<sub>10</sub> concentrations peak during winter evenings under low wind speeds suggests that residential wood combustion for home heating was the major PM<sub>10</sub> source. Where possible, these types of analyses can be combined with elemental concentrations measured from PM samples or results from receptor modeling studies to produce a 'weight-of-evidence' identification of the offending source or sources.

In Nelson Airshed B, NCC has found that high PM<sub>10</sub> concentrations, occasionally resulting in breaches of the NES, occurred under moderate to strong southwest winds, often during the spring and summer periods. This is in contrast to typical peak PM<sub>10</sub> concentrations in Nelson Airshed B, which occur during the winter when residential wood combustion for home heating is common (Davy et al. 2010). Identifying the source(s) of these peak PM<sub>10</sub> concentrations is critical for NCC to manage air quality in Airshed B. As such, the objective of this study was to identify the source(s) responsible for the non-winter peak PM<sub>10</sub> concentrations. To achieve this, advanced analyses using hourly PM<sub>10</sub> concentrations and meteorological variables were performed to gain a thorough understanding of the temporal distribution of PM<sub>10</sub> concentrations and the effects of meteorology (wind speed, wind direction) on those concentrations. Then, results from a previous receptor modeling study were used to provide 'weight-of-evidence' support for the source(s) identified as responsible for peak PM<sub>10</sub> concentrations (Davy et al. 2010).

### **1.3 REPORT STRUCTURE**

This report is comprised of 5 main chapters. Briefly, the remaining chapters have been broken down as follows:

1. Chapter 2 briefly describes the methodology and data analysis tools used in this study.
2. Chapter 3 describes the Tahunanui ambient air quality monitoring site, temporal trends in PM<sub>10</sub> concentrations and local meteorology.
3. Chapter 4 presents the results of analyses based on PM<sub>10</sub> concentrations and source contributions, and meteorological data. Implications for NCC are also discussed.
4. Chapter 5 provides concluding remarks.

## 2.0 METHODOLOGY

Hourly PM<sub>10</sub> concentrations and meteorological variables were measured at the NCC ambient air quality monitoring site at Blackwood Street, Tahunanui, Nelson. All quality assurance and quality control (QA/QC) of results and instruments was carried out by NCC and, as such, NCC maintains all QA/QC records. Figure 2.1 presents the location of the monitoring site described in this study.

This study made use of results from a previous source apportionment study in the same location (Davy et al. 2010). The methods and procedures used for the source apportionment are described in that report.

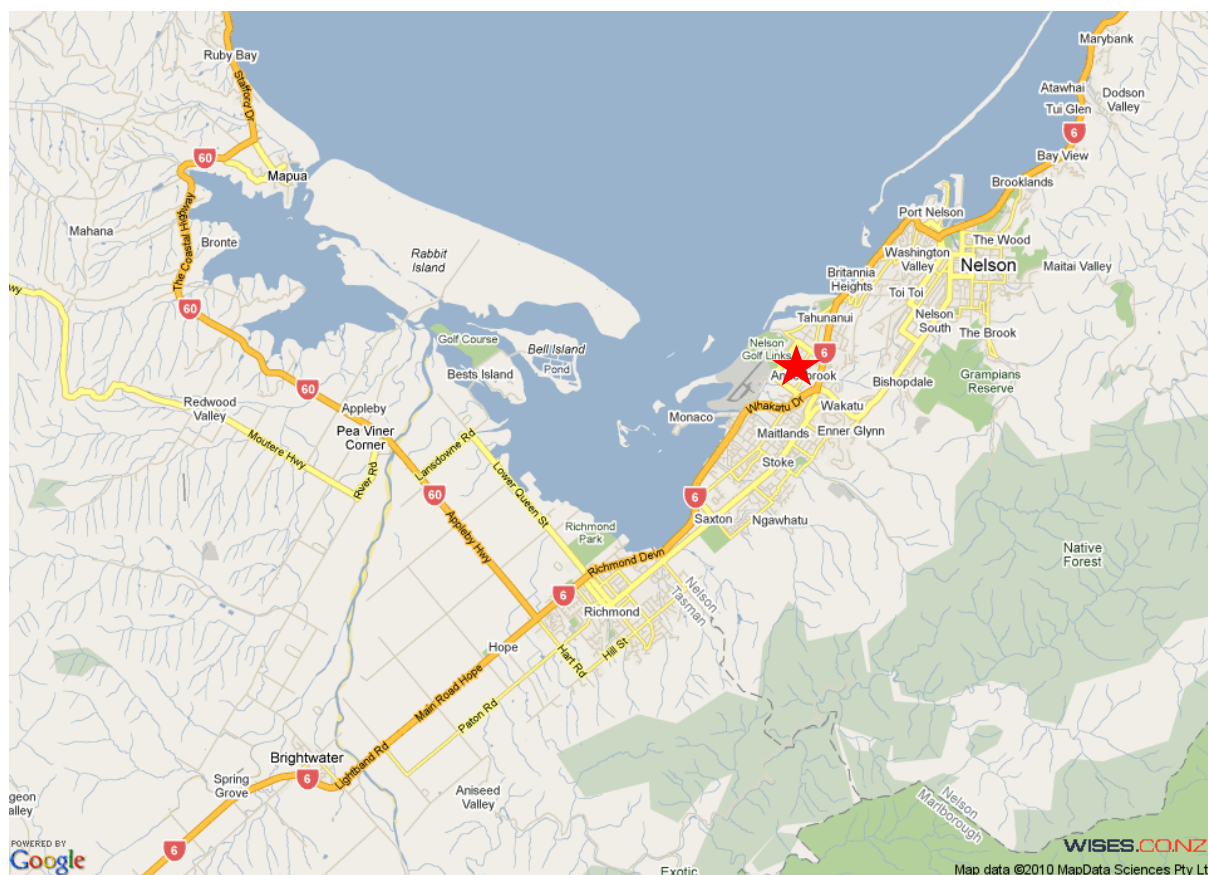


Figure 2.1 Location of the Tahunanui monitoring site in Nelson (★) (Source: Wises Maps [www.wises.co.nz](http://www.wises.co.nz))

## 2.1 DATA ANALYSIS

Hourly PM<sub>10</sub> concentrations and meteorological variables, including wind speed and direction, temperature and relative humidity, from 2007–2012 were provided by NCC. The data were analysed using the R statistical software and openair package (R Development Core Team 2011; Carslaw 2012; Carslaw and Ropkins 2012). Openair was initially developed for the analysis of air pollution measurement data and has a range of tools for importing and manipulating data and for undertaking a wide range of analyses to enhance understanding of air pollution data. Using openair, data can be analysed quickly and easily in an interactive way, allowing more time to understand and investigate the problem at hand.

Importantly, R and openair are open-source tools, meaning they are freely available to anyone in the world.

Once detailed analyses were performed using the PM<sub>10</sub> and meteorological data, data from the previous receptor modeling study were used as support to provide strong evidence for the source(s) responsible.

### 3.0 TAHUNANUI MONITORING SITE

#### 3.1 SITE DESCRIPTION

PM<sub>10</sub> concentrations were measured at an ambient air quality monitoring station located on a property off of Blackwood Street, Tahunanui in Nelson Airshed B (Lat:  $-41.2949^\circ$ , Long:  $173.2431^\circ$ , elevation: 5 m). Figure 3.1 presents the site location on a map of the local area.

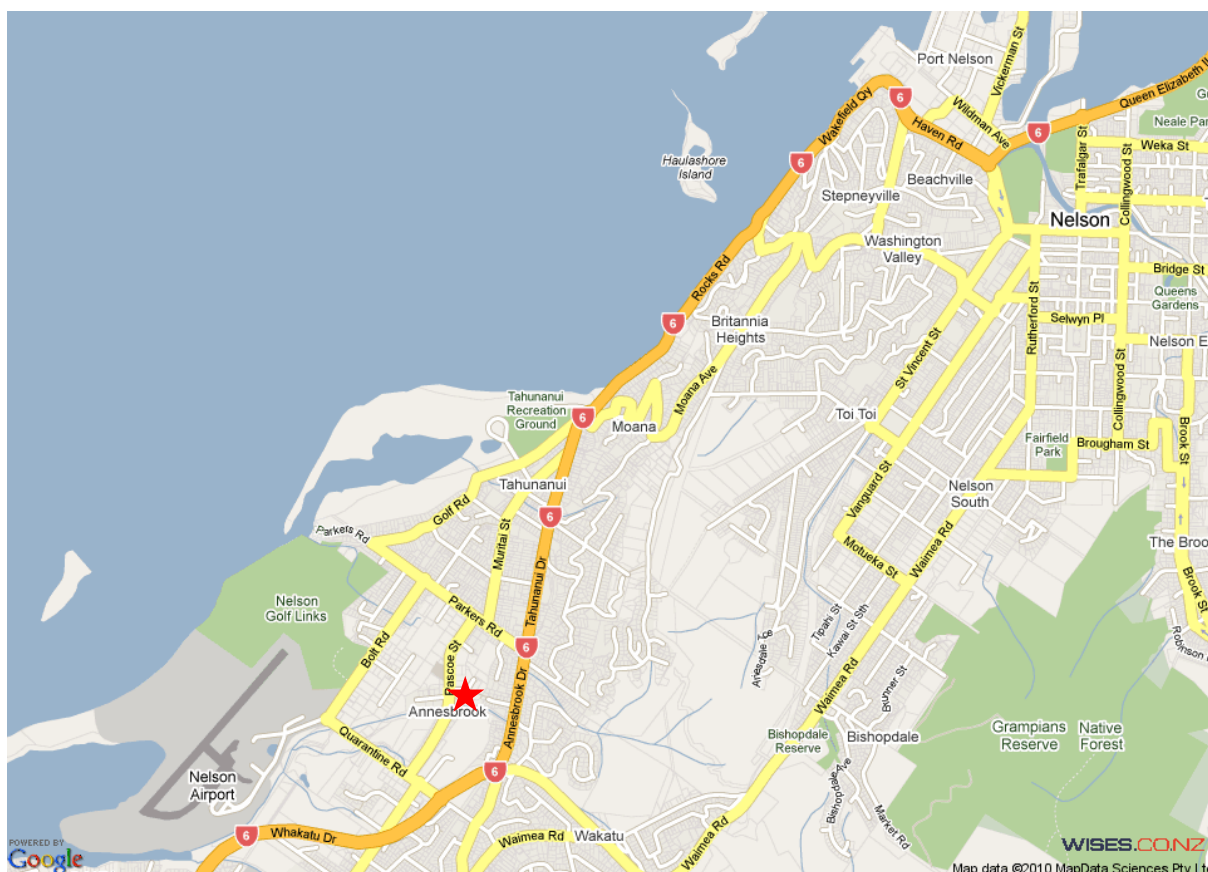


Figure 3.1 Map showing the location of the Tahunanui monitoring site (★) (Source: Wises Maps [www.wises.co.nz](http://www.wises.co.nz)).

Tahunanui is located on a narrow coastal plain bordered by hills to the east (~200–300 m high). To the north lies Tasman Bay and to the west is the Waimea Inlet. To the southwest is the Waimea Plain. The Blackwood Street site lies on the border between industrial activities to the south and west with Nelson Airport located on the edge of the Waimea Inlet west of the monitoring site. Residential activities predominate immediately to the east and north, with State Highway 6 (Annesbrook Drive) 200 m east of the site. Figure 3.2 provides an aerial photo of the Blackwood Street site and its immediate environs.



Figure 3.2 Aerial view of the NCC monitoring site (Source: Google Earth 2013).

### 3.2 PM<sub>10</sub> CONCENTRATIONS AT THE MONITORING SITE

Continuous PM<sub>10</sub> concentrations were recorded at the Tahunanui site using a Thermo-Anderson FH62 Beta-particle Attenuation Monitor (BAM), which was operated according to AS/NZS 3580.9.11.2008. Figure 3.3 presents the hourly BAM PM<sub>10</sub> monitoring results from 2008–2012. Gaps in the data were related to equipment problems. Figure 3.4 presents daily average (midnight–midnight) PM<sub>10</sub> concentrations from 2008–2012. Because few measurements were taken in 2007, that data was excluded for clarity. In Figure 3.4, a reference line at 50 µg m<sup>-3</sup> has been included to highlight the number of NES exceedances. Figures 3.3 and 3.4 highlight the seasonal patterns in PM<sub>10</sub> concentrations in Tahunanui, where peak concentrations generally occur during the winter. From Figure 3.4 it is also apparent that a number of NES exceedances occurred during the spring and summer.

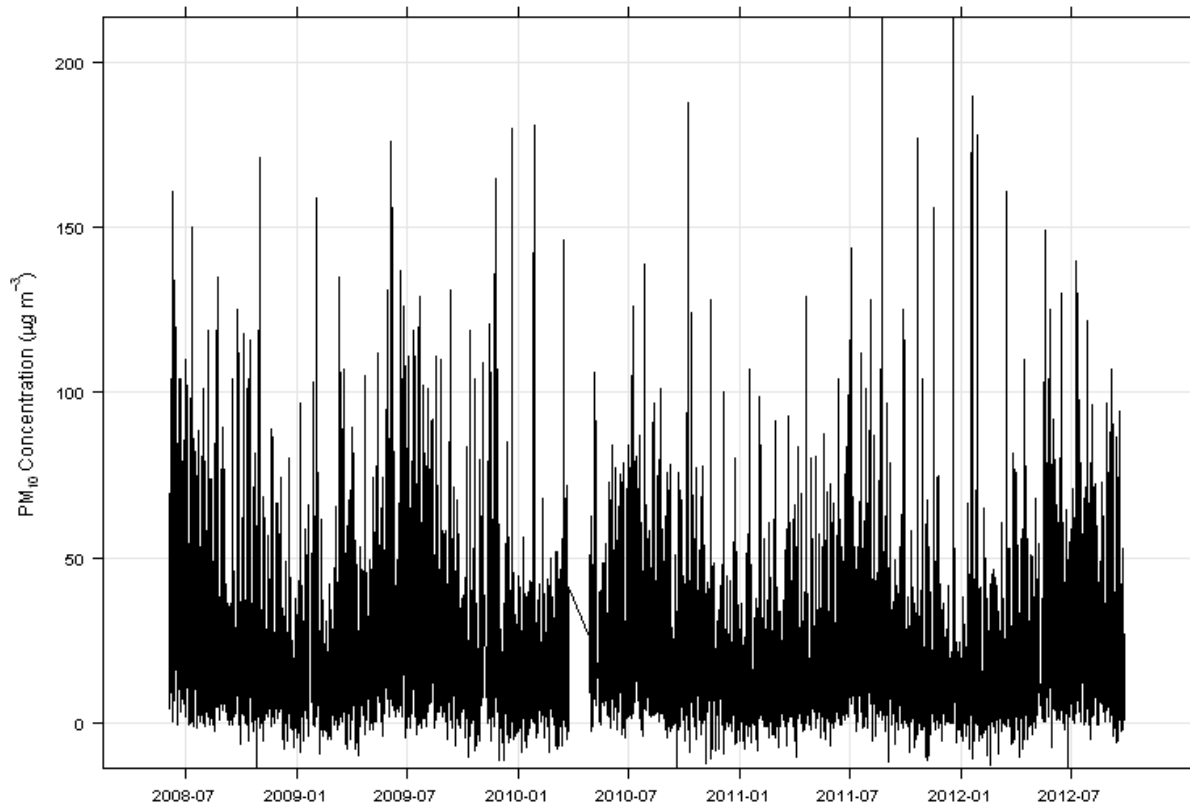


Figure 3.3 Hourly BAM PM<sub>10</sub> concentrations ( $\mu\text{g m}^{-3}$ ) at the Tahunanui site (data supplied by NCC).

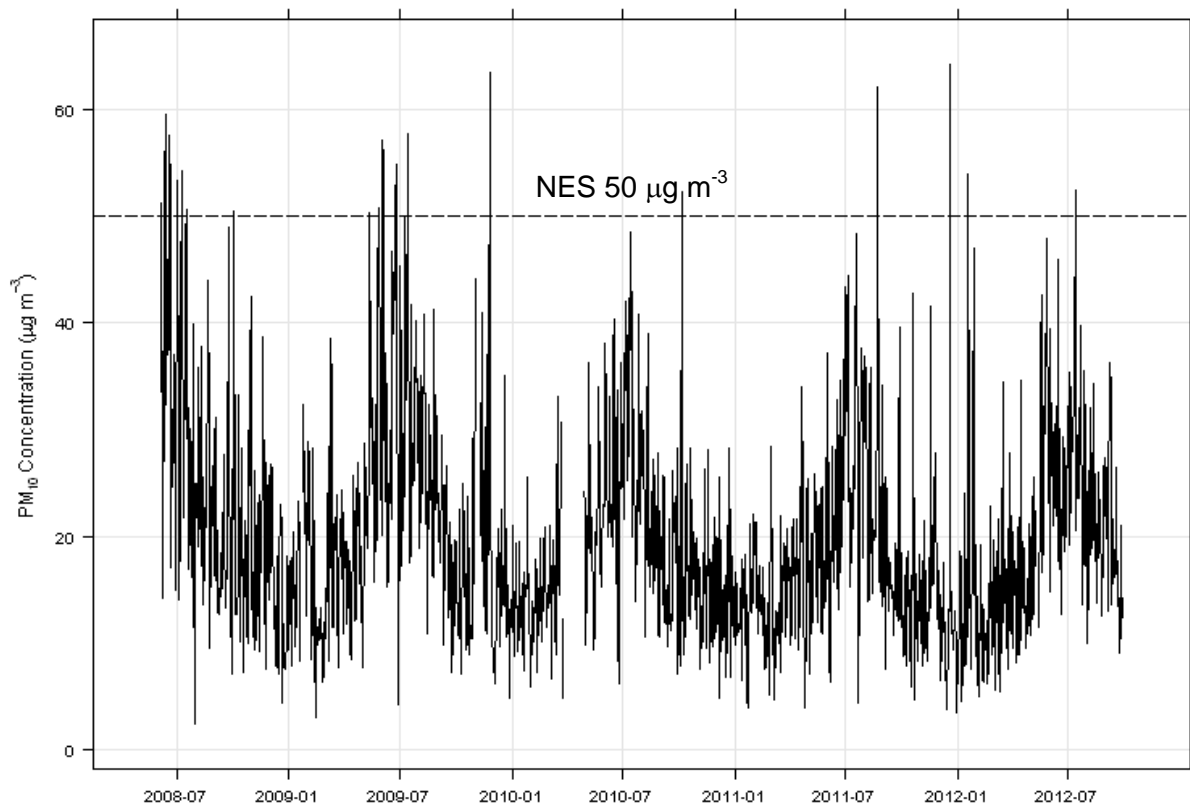


Figure 3.4 Daily BAM PM<sub>10</sub> concentrations ( $\mu\text{g m}^{-3}$ ) at the Tahunanui site. The hashed line indicates the NES value ( $50 \mu\text{g m}^{-3}$ ).

### 3.3 LOCAL METEOROLOGY AT THE TAHUNANUI SITE

A meteorological station is located at the monitoring site and is owned and operated by NCC. The predominant wind directions from 2007–2012 at Tahunanui were from the north and southeast, as shown in Figure 3.5. The meteorology at Tahunanui is defined and constrained by the local topography, with little wind from the northwesterly and easterly sectors. As shown in Figure 3.6, seasonal trends in local meteorology were apparent. During summer, winds were largely from the north, with a smaller proportion from the southeast and minor contributions from all other sectors. Conversely, winds during the winter were predominantly from the southwest to southeast, with a small northeasterly component. Interestingly, winds during spring and autumn were similar.

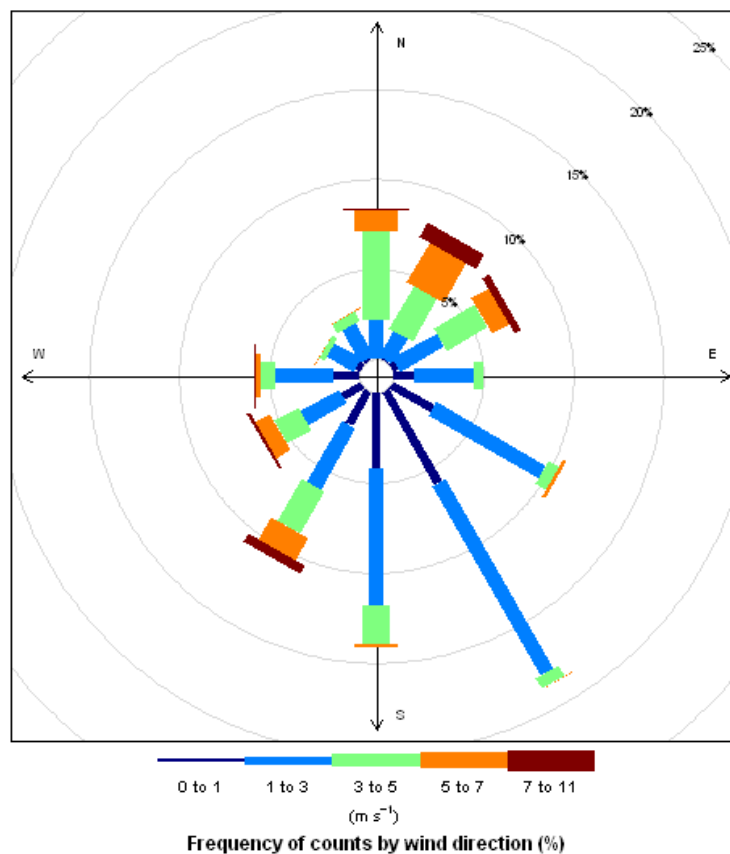


Figure 3.5 Wind rose at Tahunanui from 2007–2012.



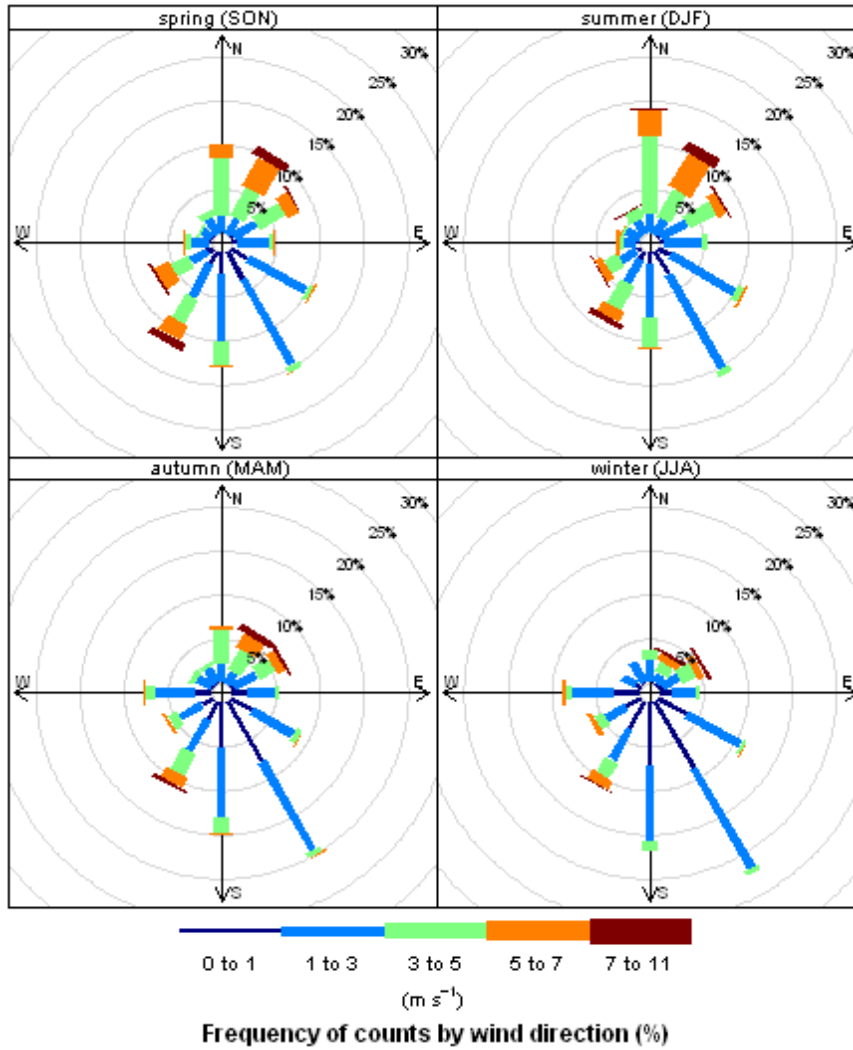


Figure 3.6 Wind roses at Tahunanui by season.

## 4.0 ANALYSES OF POLLUTION EPISODES

### 4.1 ANALYSIS OF PM<sub>10</sub> AND METEOROLOGICAL DATA

To identify the source(s) of peak PM<sub>10</sub> concentrations originating from the southwest under moderate to high wind speeds, it was necessary to identify how these conditions differed from all other conditions (wind speeds and direction). As such, average diurnal PM<sub>10</sub> concentrations were investigated as to how those PM<sub>10</sub> concentrations varied by day of the week and month. Figure 4.1 shows that PM<sub>10</sub> concentrations varied throughout each day of the week and by month using all of the available Tahunanui air quality data. Light red shading indicates the 95% confidence intervals. A number of features are immediately apparent from these plots. First, average hourly PM<sub>10</sub> concentrations show similar profiles on weekdays and very different profiles on weekends. On weekdays, PM<sub>10</sub> concentrations are highest during typical work day hours, with peak concentrations occurring between 10–11 am. A smaller evening peak in concentrations is also apparent, particularly in Figure 4.1 (b), which presents the overall average hourly PM<sub>10</sub> concentrations. The weekday/weekend difference is particularly apparent from Figure 4.1 (d), which shows that PM<sub>10</sub> concentrations are significantly higher during the week than on the weekend. These diurnal profiles and weekday/weekend differences suggest that human activities during the normal working week may be responsible for elevated PM<sub>10</sub> concentrations. If peak PM<sub>10</sub> concentrations resulted from natural phenomena then one would expect no significant difference between weekday and weekend concentrations.

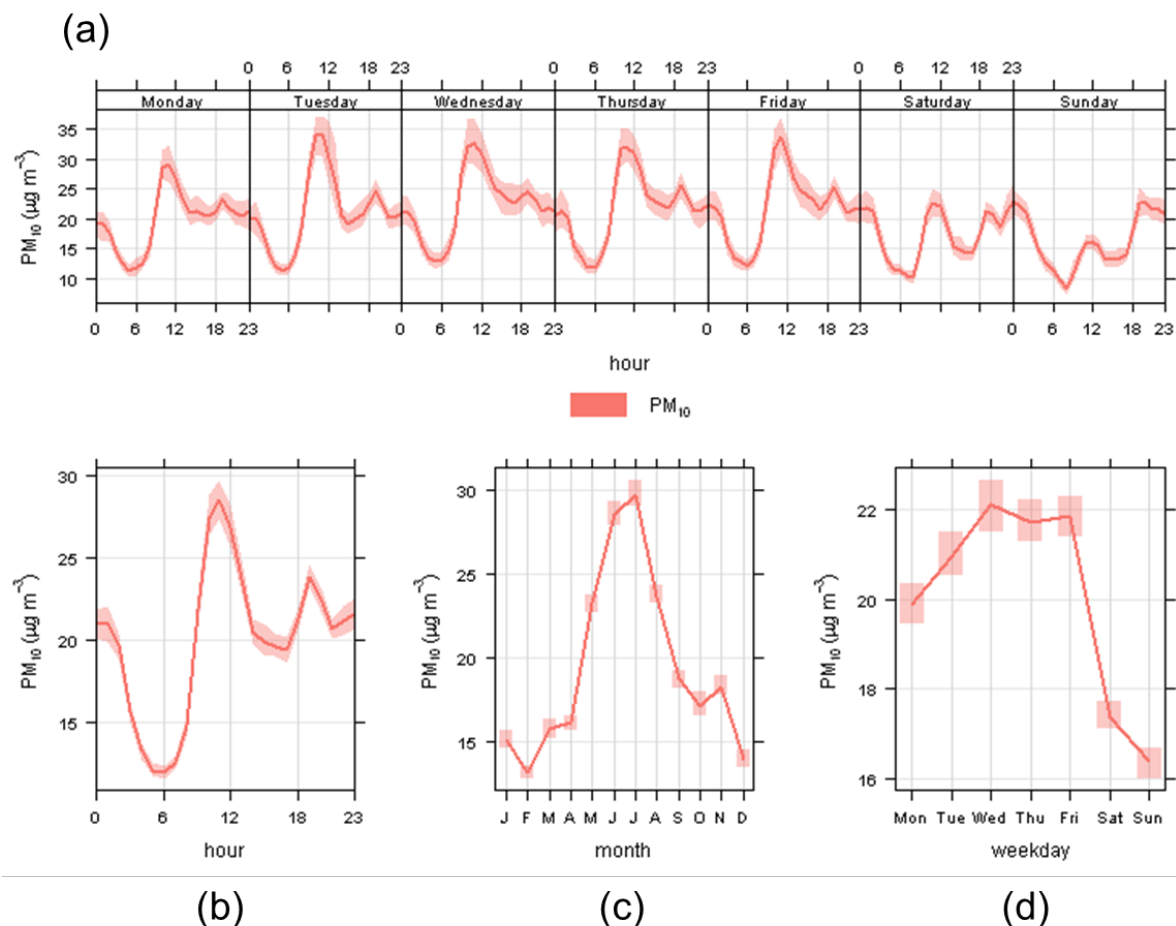


Figure 4.1 Average hourly PM<sub>10</sub> concentrations ( $\mu\text{g m}^{-3}$ ) during each day of the week (a), overall average hourly PM<sub>10</sub> concentrations ( $\mu\text{g m}^{-3}$ ) (b), average PM<sub>10</sub> concentrations ( $\mu\text{g m}^{-3}$ ) by month (c), and average PM<sub>10</sub> concentrations ( $\mu\text{g m}^{-3}$ ) by day of the week (d). Light shading indicates the 95% confidence intervals.

A second key feature from Figure 4.1 is that PM<sub>10</sub> concentrations are significantly higher during the winter months. Davy et al. (2010) found that biomass combustion for residential heating was responsible for these peaks and this explains the significant increase in PM<sub>10</sub> concentrations during colder months. It is also apparent from Figure 4.1 (c), however, that PM<sub>10</sub> concentrations increased slightly during autumn and spring compared with those during the summer months.

A previous hourly source apportionment study during the winter in Masterton found a different diurnal profile than that shown in Figure 4.1 (b) (Ancelet et al. 2012), with peak PM<sub>10</sub> concentrations occurring during the early evening (7 pm to midnight) and a smaller peak in concentrations in the morning (7–9 am). Biomass combustion for home heating was identified to be responsible for both peaks in PM<sub>10</sub> concentrations in Masterton. Based on Figure 4.1 (b), this would not be expected to be the case at Tahunanui because of the dramatic difference in diurnal profiles, where peak PM<sub>10</sub> concentrations occurred during the workday. To investigate whether the diurnal PM<sub>10</sub> profiles at Tahunanui changed during the winter similar plots to those in Figure 4.1 were prepared and are presented in Figure 4.2.

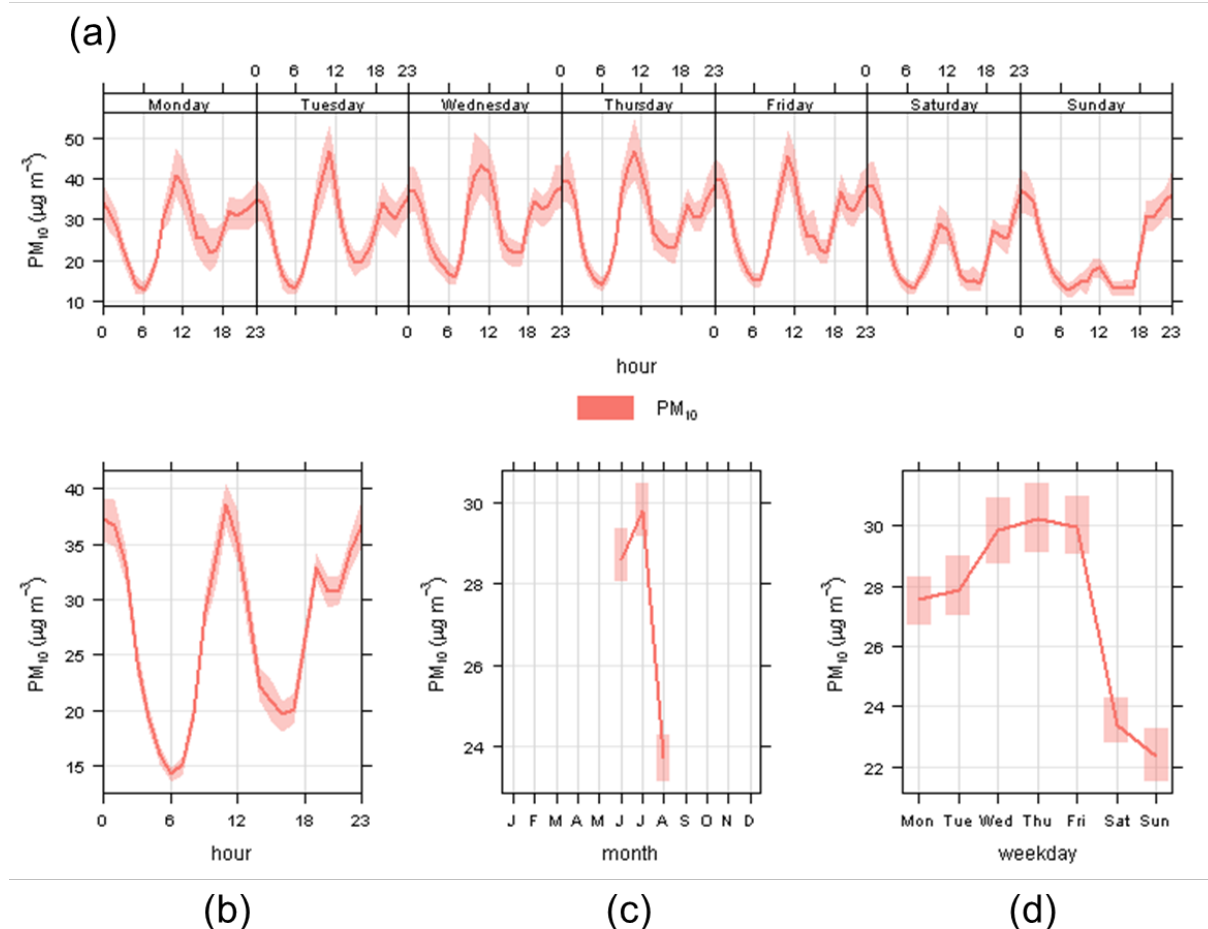


Figure 4.2 Wintertime average hourly PM<sub>10</sub> concentrations ( $\mu\text{g m}^{-3}$ ) during each day of the week (a), wintertime average hourly PM<sub>10</sub> concentrations ( $\mu\text{g m}^{-3}$ ) (b), average PM<sub>10</sub> concentrations ( $\mu\text{g m}^{-3}$ ) by month (c), and average wintertime PM<sub>10</sub> concentrations ( $\mu\text{g m}^{-3}$ ) by day of the week (d). Light shading indicates the 95% confidence intervals.

Figure 4.2 shows a marked increase in PM<sub>10</sub> concentrations during the evening, consistent with emissions from residential wood combustion. However, PM<sub>10</sub> concentrations during the work day are still higher than those during the evening on weekdays, and Figure 4.2 (d) shows that PM<sub>10</sub> concentrations during the work week are significantly higher than those during the weekend, suggesting that a source other than residential wood combustion is also a significant contributor to PM<sub>10</sub> at times.

To identify the source(s) responsible for the observed diurnal profiles and the peak non-winter PM<sub>10</sub> concentrations measured by NCC, analyses were focused on PM<sub>10</sub> concentrations when winds were from the southwest. For these analyses, wind directions were broken into quadrants, so that all wind directions from 180–270° were considered as southwesterly winds. Similarly, PM<sub>10</sub> concentration variations were examined under northeasterly, northwesterly and southeasterly wind directions. To illustrate how PM<sub>10</sub> concentrations varied according to wind direction, Figures 4.3 and 4.4 present diurnal, monthly and weekday/weekend variations from the southwesterly and all other quadrants, respectively.

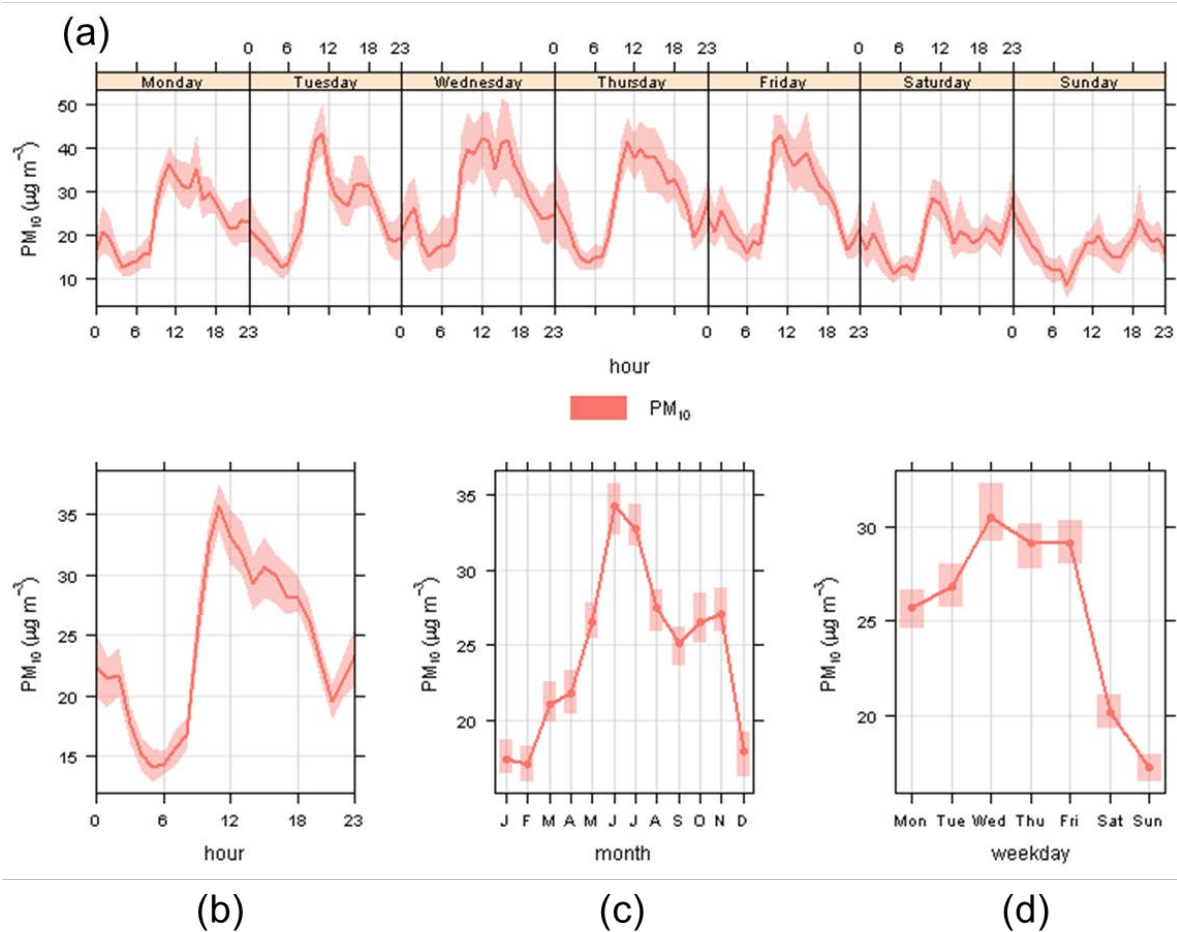


Figure 4.3 Southwesterly winds: Average hourly PM<sub>10</sub> concentrations (µg m<sup>-3</sup>) during each day of the week (a), overall average hourly PM<sub>10</sub> concentrations (µg m<sup>-3</sup>) (b), average PM<sub>10</sub> concentrations (µg m<sup>-3</sup>) by month (c), and average PM<sub>10</sub> concentrations (µg m<sup>-3</sup>) by day of the week (d) when winds were from the southwest quadrant (180–270°). Light shading indicates the 95% confidence intervals.

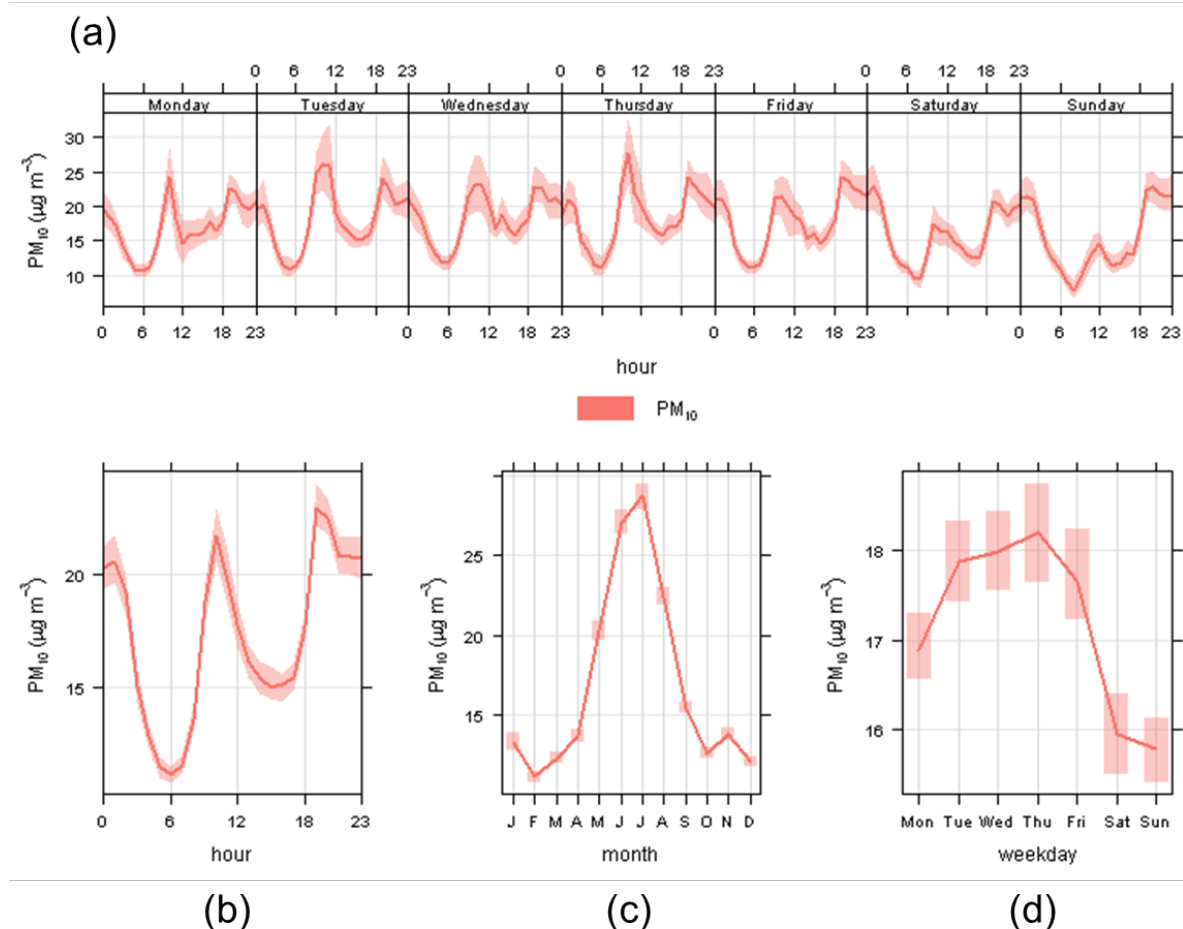


Figure 4.4 Northeastly, northwesterly and southeasterly winds: Average hourly PM<sub>10</sub> concentrations (µg m<sup>-3</sup>) during each day of the week (a), overall average hourly PM<sub>10</sub> concentrations (µg m<sup>-3</sup>) (b), average PM<sub>10</sub> concentrations (µg m<sup>-3</sup>) by month (c), and average PM<sub>10</sub> concentrations (µg m<sup>-3</sup>) by day of the week (d) when winds were from the NE, NW and SE quadrants (0–180 and 270–360°). Light shading indicates the 95% confidence intervals.

From Figures 4.3 and 4.4 it is apparent that under winds from the southwest quadrant a significant workday and weekday increase in PM<sub>10</sub> concentrations occurs when compared with winds from all other quadrants. It should also be noted that the scales in Figure 4.4 are lower than those in Figure 4.3. Based on these results, the source(s) responsible for both the observed daytime peaks in PM<sub>10</sub> concentrations and the non-winter peak PM<sub>10</sub> concentrations were strongly wind direction dependent, otherwise similar diurnal and weekday/weekend trends would be apparent from each of the wind quadrants. Nelson City Council identified that peak non-winter PM<sub>10</sub> concentrations were also associated with moderate to high wind speeds, Therefore Figure 4.5 presents PM<sub>10</sub> concentration variations when winds were from the southwest and wind speeds were greater than 3 m s<sup>-1</sup>. Figure 4.5 shows that PM<sub>10</sub> concentrations are only elevated during workdays, with peak concentrations between 10 am and 5 pm. A clear weekday/weekend difference is apparent, with weekday PM<sub>10</sub> concentrations significantly higher than those during the weekend. In contrast to Figures 4.1 and 4.2, by excluding low wind speeds from the analysis, the wintertime peak in PM<sub>10</sub> concentrations was much decreased. Elevated PM<sub>10</sub> concentrations during the winter are typically associated with low wind speeds resulting from the formation of inversion layers which limit the dispersion of pollutants (Grange et al. 2013).

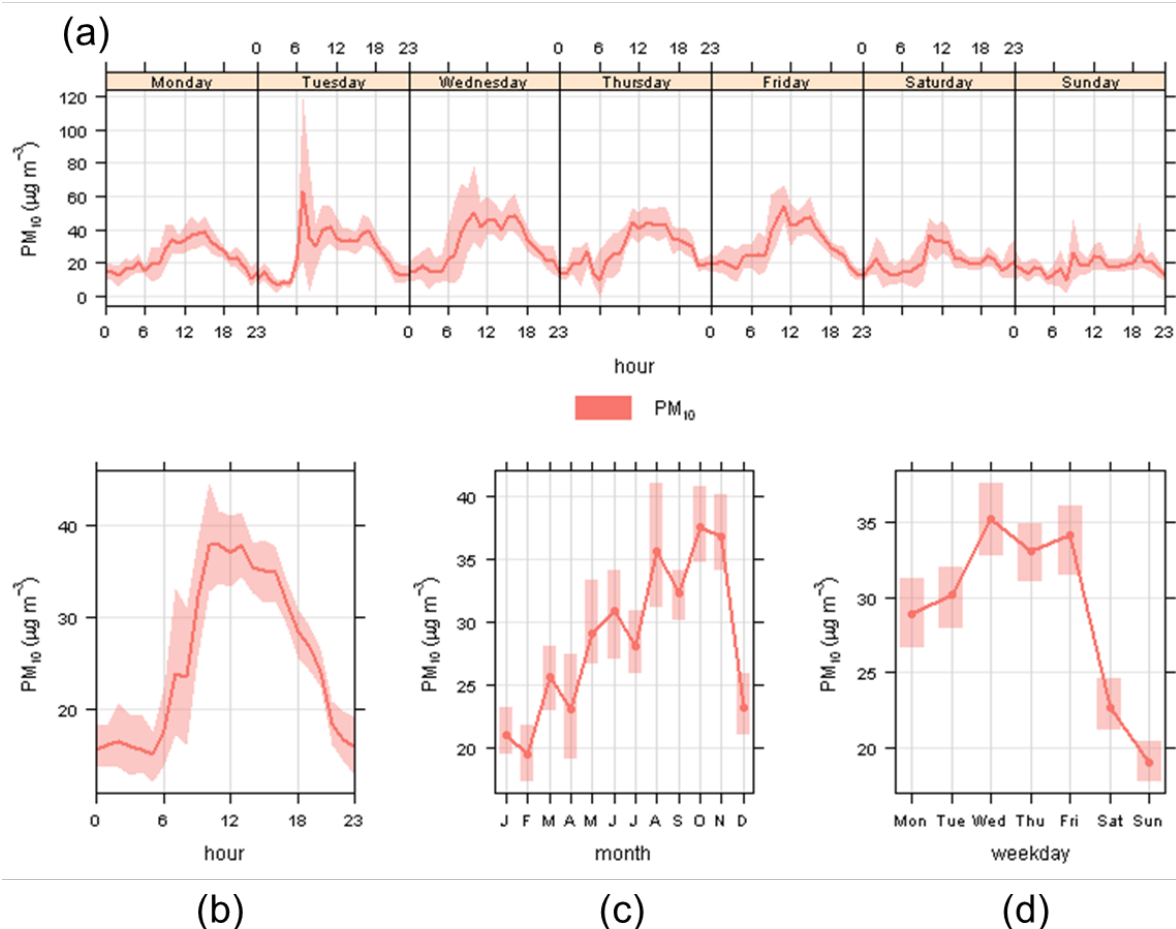


Figure 4.5 Average hourly PM<sub>10</sub> concentrations (µg m<sup>-3</sup>) under southwest winds with wind speeds greater than 3 m s<sup>-1</sup> during each day of the week (a), overall average hourly PM<sub>10</sub> concentrations (µg m<sup>-3</sup>) (b), average PM<sub>10</sub> concentrations (µg m<sup>-3</sup>) by month (c), and average PM<sub>10</sub> concentrations (µg m<sup>-3</sup>) by day of the week (d) Light shading indicates the 95% confidence intervals.

To highlight the influence of wind direction and speed on PM<sub>10</sub> concentrations at Tahunanui, Figure 4.6 presents a comparison of PM<sub>10</sub> concentrations under winds greater than 3 m s<sup>-1</sup> from the southwest with PM<sub>10</sub> concentrations under all other wind speed and direction conditions. Figure 4.6 shows that under high southwesterly winds, diurnal, weekly and seasonal PM<sub>10</sub> concentrations are dramatically different than those under other meteorological conditions, highlighting the significant influence of the source(s) located to the southwest of the sampling site.

Based on the analyses presented so far in this chapter, the source(s) of the peak PM<sub>10</sub> concentrations during southwest winds was likely to be of anthropogenic origin and appears to be associated with normal workday activities. To help identify the source(s), results from a source apportionment study (Davy et al. 2010) were analysed and the findings are presented in Section 4.2.

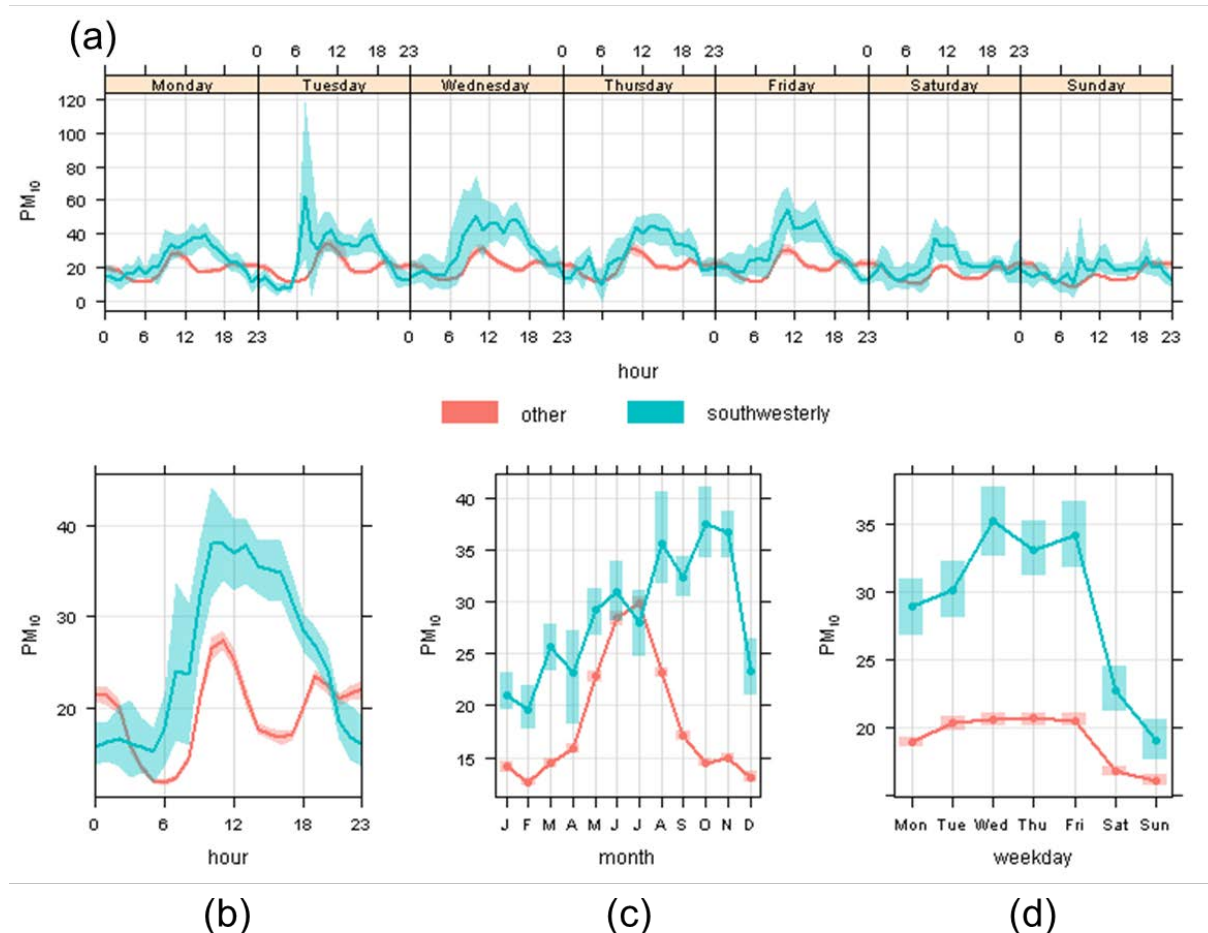


Figure 4.6 Average hourly PM<sub>10</sub> concentrations (µg m<sup>-3</sup>) under southwest winds with wind speeds greater than 3 m s<sup>-1</sup> (blue) and all other wind speeds and directions (red) during each day of the week (a), overall average hourly PM<sub>10</sub> concentrations (µg m<sup>-3</sup>) (b), average PM<sub>10</sub> concentrations (µg m<sup>-3</sup>) by month (c), and average PM<sub>10</sub> concentrations (µg m<sup>-3</sup>) by day of the week (d) Light shading indicates the 95% confidence intervals.

## 4.2 ANALYSIS USING SOURCE APPORTIONMENT STUDY RESULTS

A source apportionment study performed by Davy et al. (2010) using PM<sub>10</sub> compositional data provided information on the sources contributing to 24-hour average PM<sub>10</sub> concentrations at Tahunanui between September 2008 and September 2009. These results were used to help confirm the source(s) of non-winter peak PM<sub>10</sub> concentrations. Briefly, Davy et al. (2010) identified seven primary source contributors at Tahunanui:

1. biomass burning (emissions from solid fuel fires for home heating);
2. motor vehicles (tailpipe emissions and a road dust component)
3. secondary sulphate (from shipping emissions and natural sources);
4. marine aerosol (seasalt particles generated over the open ocean);
5. soil (crustal matter, either resuspended to the atmosphere by wind or a combination of human activities and wind);
6. surface coating activities (generated by sandblasting metal surfaces and recoating with zinc containing preparations);
7. fertiliser (an intermittent source that was associated with fertiliser storage and loading activities).



A number of these sources (biomass burning, marine aerosol and surface coating activities) are unlikely to be responsible for the peak  $PM_{10}$  concentrations measured at Tahunanui because they were not found to originate from the southwest or were associated with low wind speed conditions. However, for assurance, contributions from these sources were also included in analyses.

Using openair, hourly wind speeds and directions were converted to daily averages using a vector averaging procedure. A full description of this process can be found in the openair manual (Carslaw 2012). Using the vector averaged wind directions, wind speeds and  $PM_{10}$  source contributions, analyses were performed as to how source contributions varied by wind direction. Similar to Chapter 4.1, wind directions were grouped into quadrants, with winds from  $180\text{--}270^\circ$  considered to be southwesterly (northwest =  $270\text{--}360^\circ$ ; northeast =  $360\text{--}90^\circ$ ; southeast =  $90\text{--}180^\circ$ ). Motor vehicle and soil source contributions were identified to be strongly influenced by southwesterly winds. Figures 4.7 and 4.8 present scatterplots of motor vehicle and soil contributions, respectively, from the southwest quadrant and from all of the other quadrants. As comparisons, similar scatterplots for sulphate and surface coating contributions are shown in Figures 4.9 and 4.10, respectively. Marine aerosol and biomass burning contributions were also not strongly influenced by southwesterly winds. The fertiliser source identified by Davy et al. (2010) also showed southwesterly wind dependence, but the intermittent nature of the source would not produce the  $PM_{10}$  concentration profiles presented in Chapter 4.1 and therefore activities associated with the loading and unloading of fertiliser are not considered responsible for the regular peak  $PM_{10}$  concentrations from the southwest at Tahunanui.

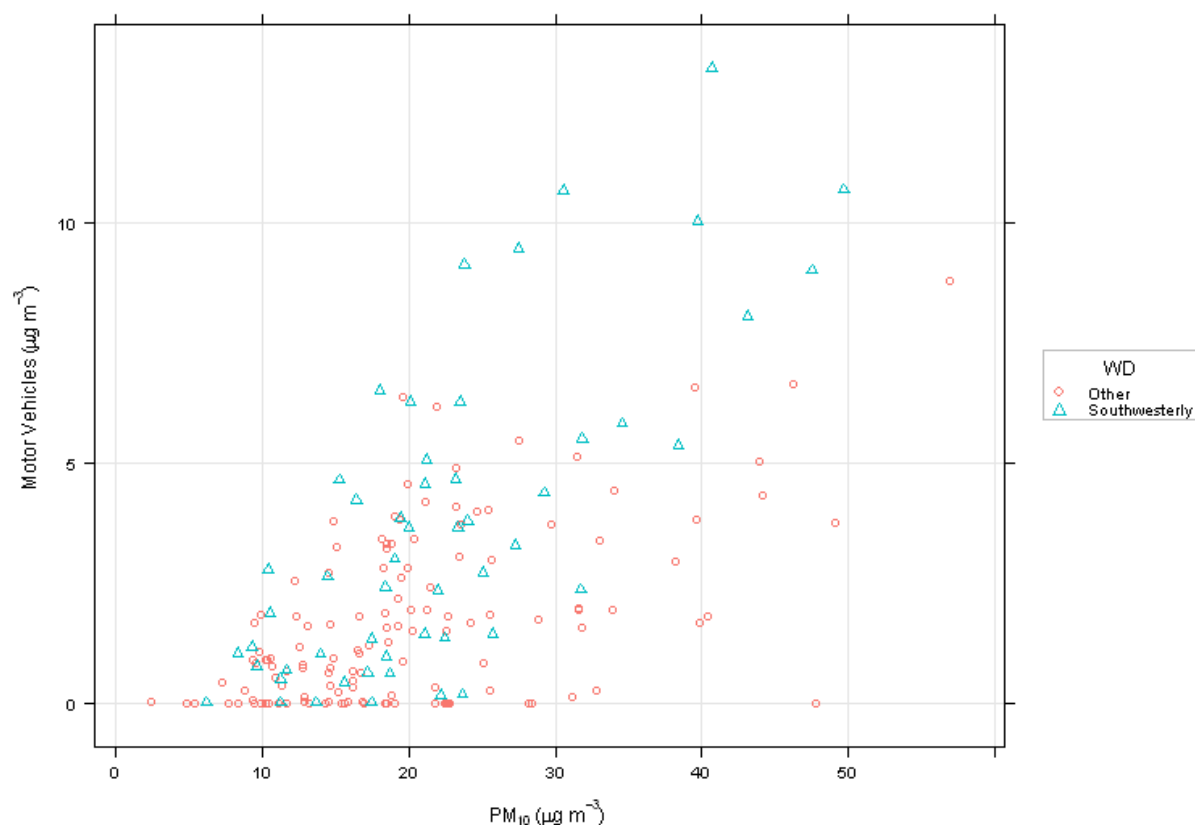


Figure 4.7 Scatterplot of motor vehicle contributions ( $\mu\text{g m}^{-3}$ ) versus  $PM_{10}$  concentrations ( $\mu\text{g m}^{-3}$ ) under winds from the southwest (blue) and all other wind quadrants (red).

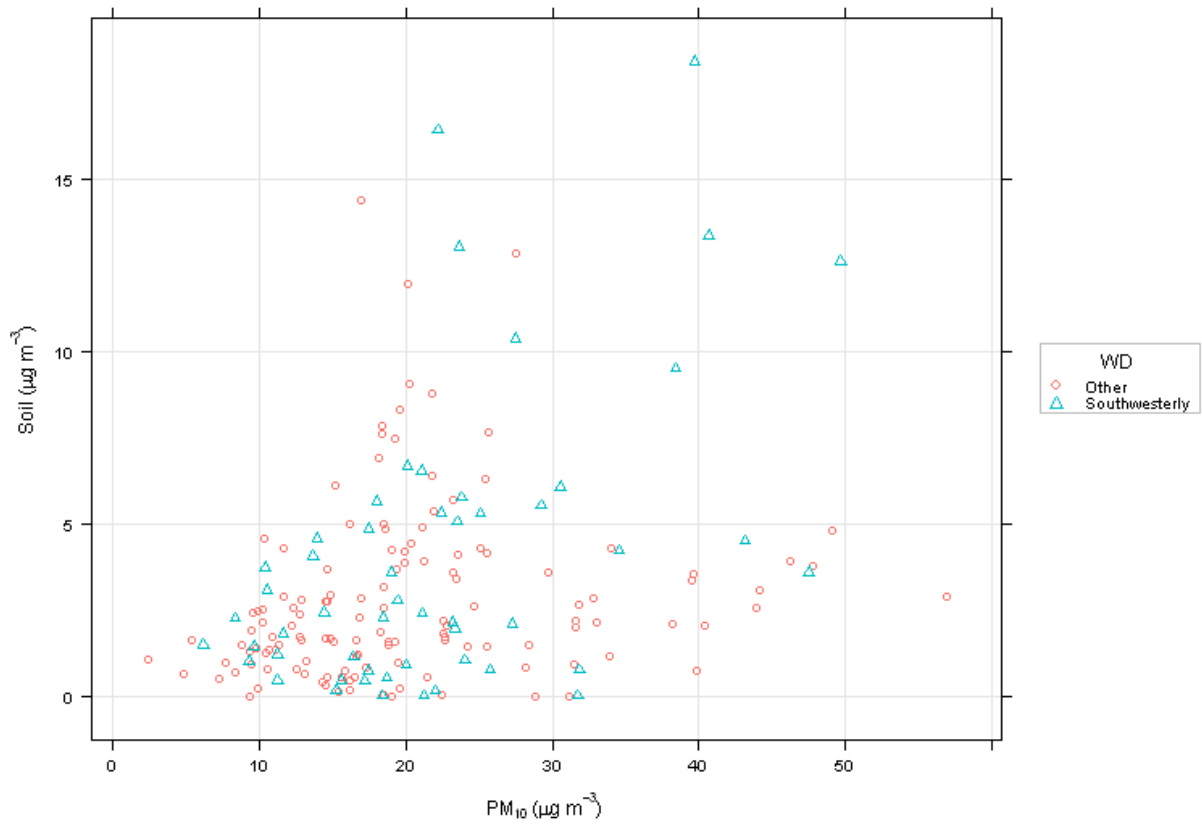


Figure 4.8 Scatterplot of soil contributions ( $\mu\text{g m}^{-3}$ ) versus PM<sub>10</sub> concentrations ( $\mu\text{g m}^{-3}$ ) under winds from the southwest (blue) and all other wind quadrants (red).

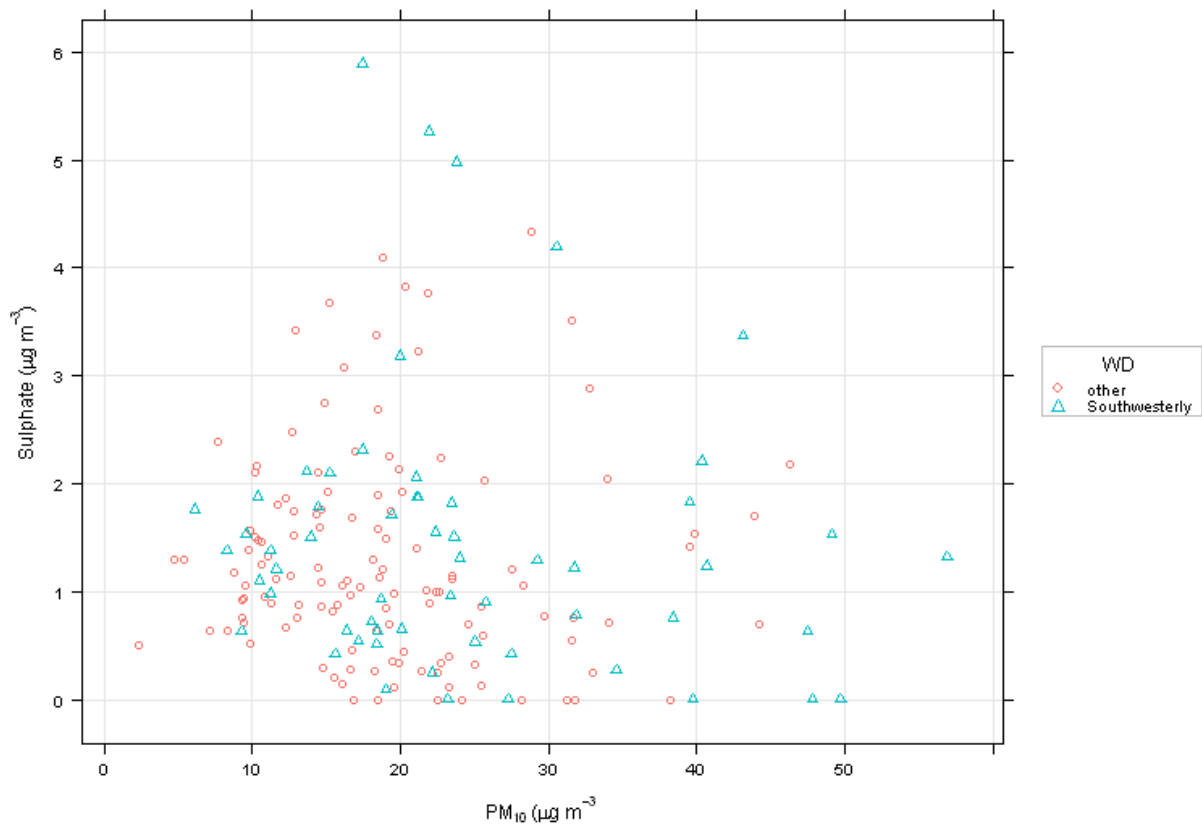


Figure 4.9 Scatterplot of sulphate contributions ( $\mu\text{g m}^{-3}$ ) versus PM<sub>10</sub> concentrations ( $\mu\text{g m}^{-3}$ ) under winds from the southwest (blue) and all other wind quadrants (red).

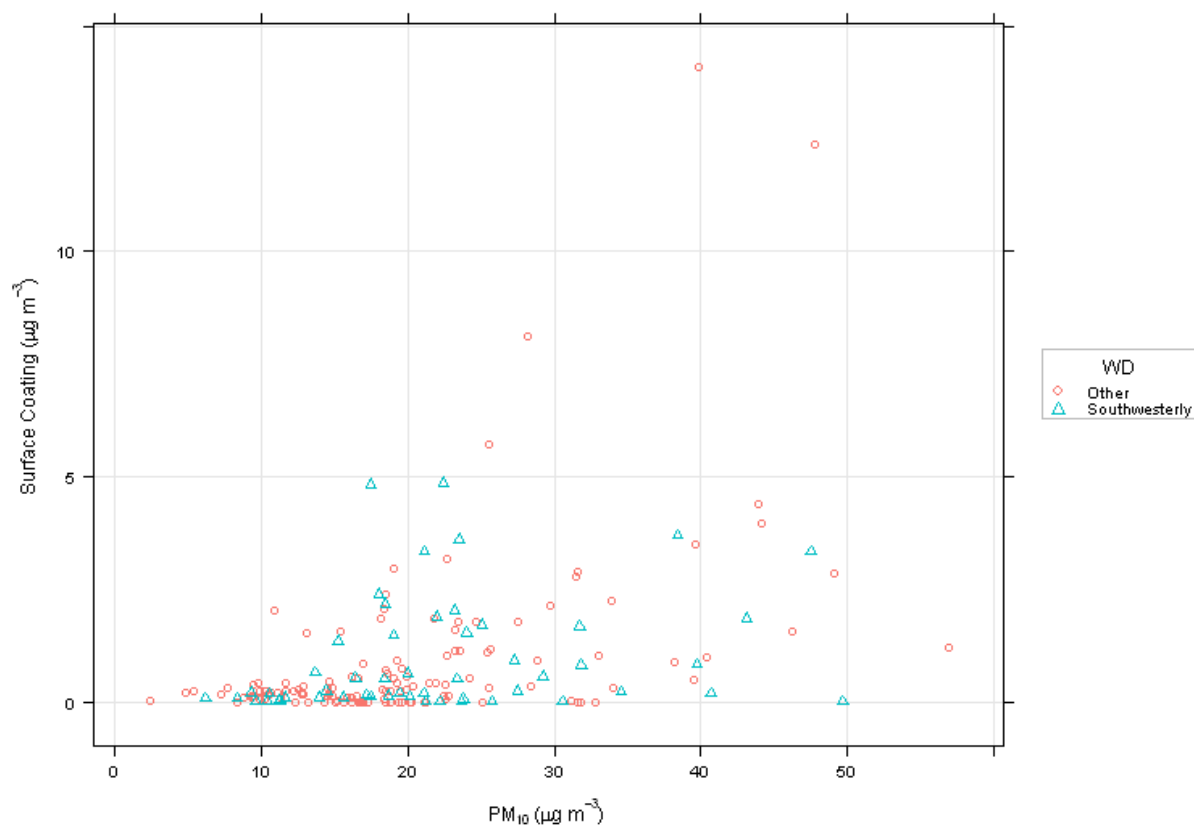


Figure 4.10 Scatterplot of surface coating activity contributions ( $\mu\text{g m}^{-3}$ ) versus PM<sub>10</sub> concentrations ( $\mu\text{g m}^{-3}$ ) under winds from the southwest (blue) and all other wind quadrants (red).

The good correlations of the soil ( $r^2 = 0.35$ ) and motor vehicle ( $r^2 = 0.52$ ) source contributions with winds from the southwest is in agreement with the conclusion from Chapter 4.1 that the peak PM<sub>10</sub> concentrations during southwest winds were likely to be of anthropogenic origin and appears to be associated with normal workday activities. The association of soil and vehicular sources of PM<sub>10</sub> originating from the southwest suggests that it is vehicular movements on unsealed yards or roadways in the industrial area that are responsible for the peak PM<sub>10</sub> concentrations. The association of soil and motor vehicles indicates that along with vehicular tailpipe emissions, vehicle movements and wind-action re-suspend dust from unsealed yards and other roadways to produce high contributions from soil. In fact, Davy et al. (2010) suggested that the relatively high soil contribution and similar vehicular and soil source profiles at Tahunanui were the result of mixed profiles resulting from traffic movements in the industrial area southwest of the Tahunanui air quality monitoring site. Since it is likely that the majority of soil was the result of re-entrainment by vehicles, the motor vehicle and soil source contributions were combined to produce a scatterplot under southwesterly and all other wind directions (Figure 4.11). Figure 4.11 shows that PM<sub>10</sub> associated with motor vehicle emissions and crustal matter from the industrial area to the southwest of the Tahunanui monitoring site are most likely responsible for the observed PM<sub>10</sub> concentration profiles (Section 4.1) and the non-peak PM<sub>10</sub> concentrations recorded by NCC because of their strong correlation with southwesterly winds ( $r^2 = 0.59$ ). When only elemental concentrations were used to derive a soil contribution (using reconstructed mass calculations shown explicitly in Davy et al. (2010)), a similar plot to Figure 4.11 arises under winds from the southwesterly quadrant (Figure 4.12).

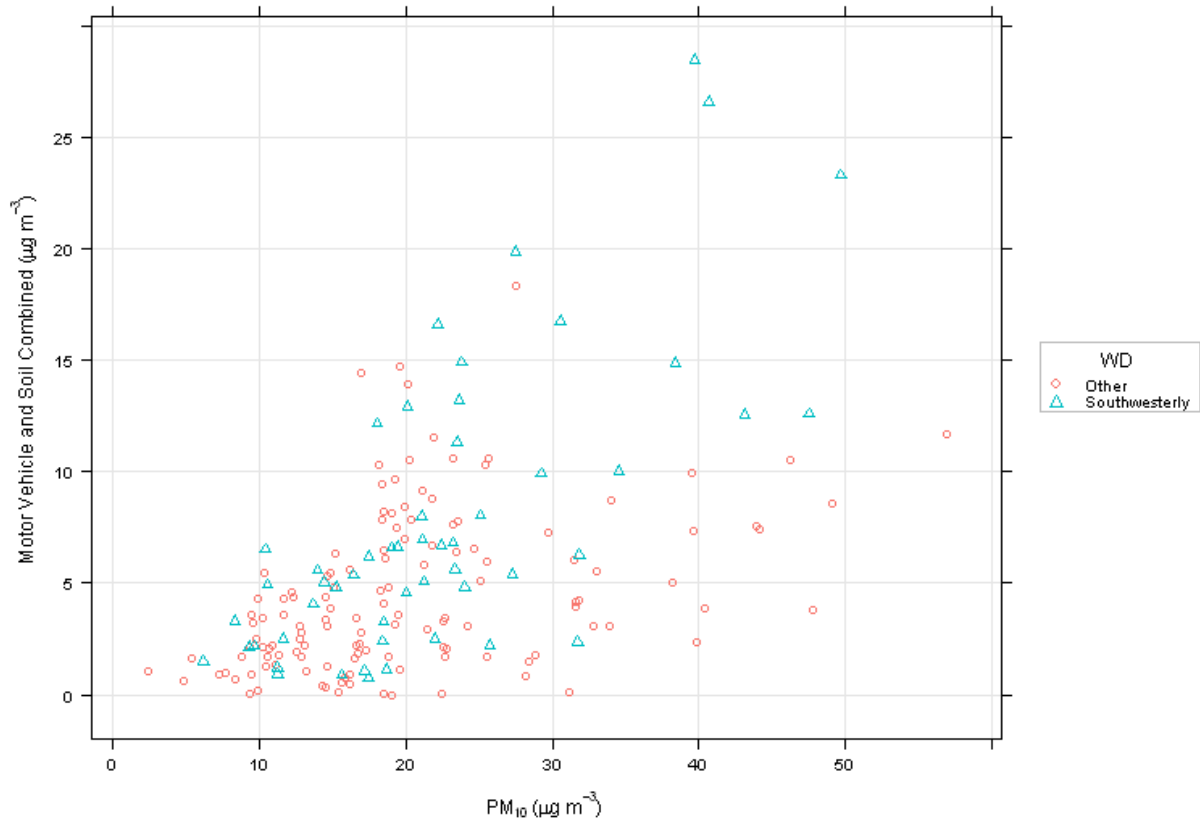


Figure 4.11 Scatterplot of motor vehicle and soil contributions combined ( $\mu\text{g m}^{-3}$ ) versus  $\text{PM}_{10}$  concentrations ( $\mu\text{g m}^{-3}$ ) under winds from the southwest (blue) and all other wind quadrants (red).

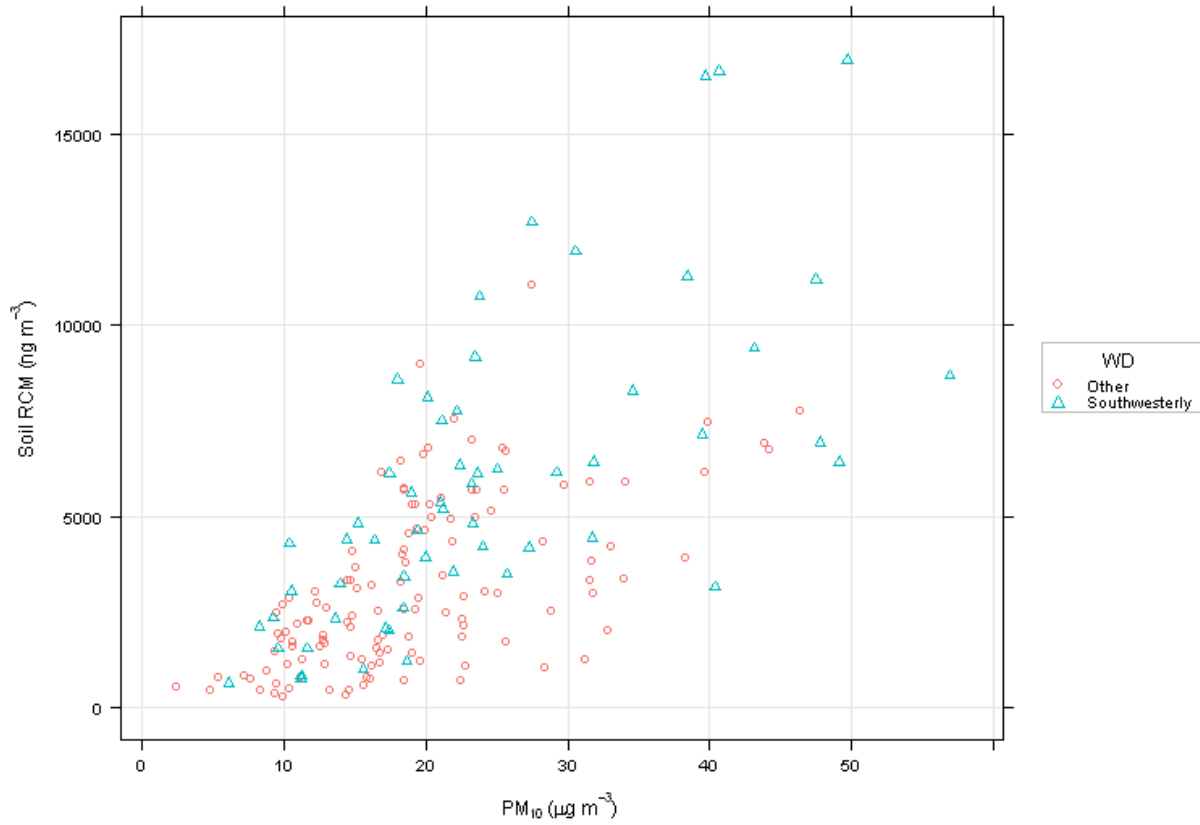


Figure 4.12 Scatterplot of soil contributions ( $\text{ng m}^{-3}$ ) calculated from mass reconstruction versus  $\text{PM}_{10}$  concentrations ( $\mu\text{g m}^{-3}$ ) under winds from the southwest (blue) and all other wind quadrants (red).

### **4.3 IMPLICATIONS FOR NELSON CITY COUNCIL**

The results of the analyses presented in this chapter indicate that it is likely that movements of vehicles on unsealed yards or other roadways associated with industrial activities have a significant impact on air quality in Nelson Airshed B. As such, appropriate management of PM emissions from these activities is likely to improve local air quality and would reduce the number of PM<sub>10</sub> NES exceedances experienced at Tahunanui outside of the wintertime domestic fire season.

## **5.0 SUMMARY OF THE ANALYSIS OF PM<sub>10</sub> CONCENTRATIONS AT TAHUNANUI**

Meteorological and PM<sub>10</sub> concentration data from 2008–2012 were used in conjunction with source apportionment data from a previous study (Davy et al. 2010) to identify the source(s) of peak PM<sub>10</sub> concentrations at Tahunanui that occurred under moderate to high wind speeds from the southwest. It was also found that these peak PM<sub>10</sub> episodes only occurred during normal weekday working hours and were generally absent during the weekend, ruling out the possibility that it was entirely due to natural phenomena which would be equally likely to occur during the week or weekend. Detailed analyses identified that the PM<sub>10</sub> particles were largely composed of crustal matter (soil) and that the source of these PM<sub>10</sub> concentrations was likely to be the movement of vehicles around an industrial area to the southwest of the monitoring site. These vehicle movements not only produced direct (tailpipe) emissions, but also re-entrained dust from unsealed yards or other roadways to the atmosphere. Combining the soil and motor vehicle contributions from the source apportionment study produced a strong correlation with winds from the southwest. Importantly, the anthropogenic nature of this PM<sub>10</sub> source suggests that emissions from these activities could be managed by Nelson City Council.

## 6.0 REFERENCES

Ancelet, T., Davy, P. K., Mitchell, T., Trompetter, W. J., Markwitz, A. & Weatherburn, D. C. Identification of Particulate Matter Sources on an Hourly Time-Scale in a Wood Burning Community. *Environmental Science & Technology* 46, 4767-4774 (2012).

Carslaw, D. & Ropkins, K. openair — An R package for air quality data analysis. *Environmental Modelling & Software* 27-28, 52-61 (2012).

Carslaw, D. The openair manual - open-source tools for analysing air pollution data. Manual for version 0.7-0 1-254 (King's College London, 2012).

Davy, P., Trompetter, B. & Markwitz, A. Source apportionment of PM10 at Tahunanui, Nelson. GNS Science Consultancy Report 2010/198 1-71 (2010).

Grange, S. K., Salmond, J. A., Trompetter, W. J., Davy, P. K. & Ancelet, T. Effect of atmospheric stability on the impact of domestic wood combustion to air quality of a small urban township in winter. *Atmospheric Environment* 70, 28-38 (2013).

Krzyzanowski, M. & Cohen, A. Update of WHO air quality guidelines. *Air Quality, Atmosphere & Health* 1, 7-13 (2008).

R Development Core Team, 2011. R: A Language and Environment for Statistical Computing. R Foundation for Statistical Computing, Vienna, Austria, ISBN 3-900051-07-0.